Quantifying encoding redundancy induced by rate correlations in Poisson neurons

Tim Herfurth and Tatjana Tchumatchenko
Max Planck Institute for Brain Research, Theory of Neural Dynamics, Max-von-Laue-Strasse 4, 60438 Frankfurt, Germany

(Received 14 August 2018; revised manuscript received 28 January 2019; published 2 April 2019)

Temporal correlations in neuronal spike trains are known to introduce redundancy to stimulus encoding. However, exact methods to describe how these correlations impact neural information transmission quantitatively are lacking. Here, we provide a general measure for the information carried by correlated rate modulations only, neglecting other spike correlations, and use it to investigate the effect of rate correlations on encoding redundancy. We derive it analytically by calculating the mutual information between a time-correlated, rate modulating signal and the resulting spikes of Poisson neurons. Whereas this information is determined by spike autocorrelations only, the redundancy in information encoding due to rate correlations depends on both the distribution and the autocorrelation of the rate histogram. We further demonstrate that at very small signal strengths the information carried by rate correlated spikes becomes identical to that of independent spikes, in effect measuring the signal modulation depth. In contrast, a vanishing signal correlation time maximizes information but does not generally yield the information of independent spikes. Overall, our study sheds light on the role of signal-induced temporal correlations for neural coding, by providing insight into how signal features shape redundancy and by establishing mathematical links between existing methods.

DOI: 10.1103/PhysRevE.99.042402

I. INTRODUCTION

A long-standing challenge in neuroscience has been to understand the code that is used in sequences of stereotyped action potentials (spike trains) to transmit information about relevant signals. Earlier studies have suggested that the efficiency of the neural code can be increased when temporal correlations in the spike trains are minimized, or equivalently, that temporal correlations in spike trains introduce redundancy to signal encoding [1–4]. This coding redundancy among spikes can be quantified as the (negative) difference between the mutual information in spikes about a signal that is carried by the spike trains as a whole (I_{corr}) and the one carried by their individual spikes, if they are treated as being independent (I_{ind}) [1,5,6]. However, exact methods to simultaneously determine both quantities were lacking until recently and therefore quantifying the effect of temporal spike correlations on coding redundancy remained an open challenge.

A method to determine I_{ind} has been known for a while and provides a mathematically tractable information measurement that only requires knowledge of the rate variations induced by the signal under consideration [1,7]. It has been used to analyze information transmission in various brain regions such as hippocampus [8–12], visual cortex [13], and the fly visual system [1]. However, I_{ind} does not account for rate correlations or any other spike correlations; and calculating the full information I_{corr} between spike trains and signals under consideration of spike correlations has been a major obstacle. Accordingly, most of the analytic methods are based on approximations or reduced features of the spike trains (see, e.g., [14–20]). An exact but computationally expensive and numerically sensitive method was introduced by Strong *et al.* [21–23]. Similarly, previous studies that have directly computed the synergy and redundancy resulting from spike correlations either relied on series expansion approximations [1,24–27] or were formulated in terms of probability distributions that are not generally known if temporal precise spiking is included [28] (see [6,29] for reviews and Sec. IV for details).

However, an exact method to calculate I_{corr} based on two-point correlation functions has been put forward recently [30]. Importantly, this method fully captures the effect of all temporal correlations that are present. Now, systematically comparing I_{ind} and I_{corr} for a given scenario enables an analytical investigation of the role of spike correlations—both intrinsic and signal-induced—for encoding redundancy. Analyzing how I_{ind} and I_{corr} are shaped by stimulus features yields further insights into the mechanisms that underlie encoding redundancy and hence are critical for optimization in encoding performance. Here, we address two open questions: How can the impact of different temporal spike correlation structures on coding redundancy be quantified? And what are the properties of a rate code that determine these effects?

We analyze how different signal properties and temporal spike correlations shape the information contained in correlated and independent spikes (the terms "independent spikes" and "correlated spikes" are used in this short form for brevity; they refer to cases where spikes are *treated as* being independent or correlated, respectively). We focus on the effects of rate correlations, in particular temporal spike correlations that are signal induced, e.g., by sensory inputs, and do not stem from intrinsic dynamics or spontaneous activity. We thereby establish mathematical links between information theoretical methods with and without incorporation of temporal spike correlations [1,5,31].

We consider Poisson neurons whose rate follows and represents a signal. We chose this approach for several reasons: Poisson firing can account well for the irregular firing pattern and noise characteristics of cortical neurons [32–38].

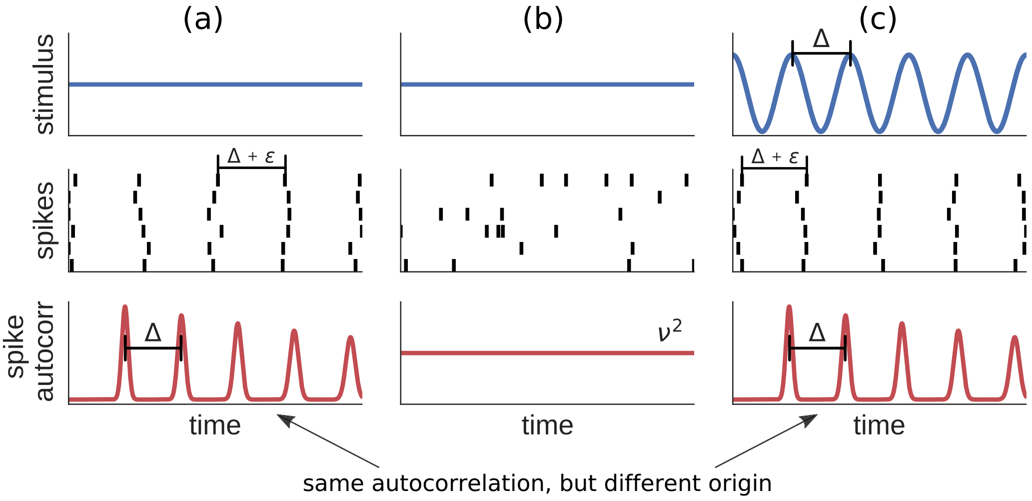

FIG. 1. Spike autocorrelations can emerge from intrinsic neural dynamics or can be signal induced, or may not be present at all. Here, we illustrate these scenarios. (a) Intrinsic correlations. A constant signal (top) causes regular spiking responses with only small variations ϵ in the interspike intervals (middle). This could represent an integrate-and-fire neuron that is stimulated by a constant suprathreshold current and weak noise. The resulting temporal autocorrelation of the spike trains shows oscillations (bottom). (b) Absence of temporal correlations. Poisson neurons responding to a constant signal at constant rate have independent interspike intervals. (c) Signal-induced correlations. An oscillating stimulus induces regular interspike intervals (here, neurons fire around the peaks of the stimulus). Even though the spiking correlations (bottom) look similar to those in (a), they are induced by signal-induced rate correlations rather than internal dynamics. In this article, we examine the effect of rate correlations on information transmission.

Poisson neurons do not exhibit intrinsic spike correlations and therefore are eligible to analyze signal-induced correlations (see Fig. 1). Furthermore, the Poisson distribution is mathematically tractable and allows for analytic calculations [7,36,39]. Importantly, in our methodical framework the information measure derived for Poisson neurons is also expedient for non-Poisson spiking neurons where it can be used to dissect the effects of intrinsic and signal-induced rate correlations.

Using analytic calculations, we derive an expression that yields the complete information I_{corr} contained in rate modulations and neglects the effects of intrinsic correlations, as is naturally given for Poisson neurons. This information can be determined using the spike train autocorrelation irrespective of the rate distribution. This is in contrast to the information in independent spikes (I_{ind}) which is determined by the distribution of firing rates across time only. Moreover, using three example signal processes we confirm that the information in independent spikes is an upper bound for the information in correlated spikes, reflecting a previously stated redundancy among spikes [1]. We further find that I_{ind} and I_{corr} become identical in the limit of vanishing rate modulations. In this case the variance of the firing rate across time completely determines information transmission. We also demonstrate that signals with a vanishing correlation time (a flat spectrum) maximize the information in correlated spikes but surprisingly do not generally lead to independent spikes even in Poisson neurons, indicating that the approximation of independent spikes and vanishing signal correlations are not equivalent in terms of information transmission.

Our study provides interesting results regarding the differences in information carried by spikes when they are assumed independent and the information in correlated spikes. Moreover, we provide a general framework for computing the redundancy in the neural code dissecting the effects of rate correlations and other temporal correlations.

II. RESULTS

To quantitatively analyze the impact of temporal spike correlations on information transmission we consider Poisson neurons whose firing rate $r(t)$ follows a time-dependent signal $s(t)$, which implies a rate encoding of the signal. In the notation of this work $s(t) = r(t)$ is assumed, which introduces an equivalence of the signal and rate trajectories. Temporal correlations in the firing rate are then given by the temporal correlations in the signal. Generally, our results are also valid for other homeomorphic rate functions $r(s(t))$, where the rate trajectory can be considered to be the signal itself. Rate correlations in this case may not be exclusively signal induced. The choice of Poisson neurons allows us to specifically investigate the effect of these signal-induced correlations only since intrinsic spike correlations are not present (see Fig. 1). In Sec. II A we review the expressions for the mutual information between signal and spikes with and without consideration of temporal correlations. By means of three example rate processes—a telegraph process, a process with uniform rate distribution, and an Ornstein-Uhlenbeck process—we demonstrate how overall rate distribution and correlation structure of these processes influence the two information measures, and by contrasting both measures we investigate the role of temporal correlations for coding redundancy (Sec. II B). Moreover, we link the information transmission of independent and correlated spikes and show that both information measures are equivalent in the regime of small rate modulations (Sec. II C) where only the average modulation depth determines information content in both cases. Finally, in Sec. II D we present that vanishing signal or rate correlation times do not correspond to entirely independent spikes but maximize the information in correlated spikes.

A. Information carried by independent and correlated spikes in Poisson neurons

The information carried by (assumedly) *independent* spikes that are generated via point processes with time-dependent firing rate $r(t)$ has been found to be [1,7]

$$I_{\text{ind}} = \frac{1}{T}\int_0^T dt \frac{r(t)}{\nu} \log_2 \frac{r(t)}{\nu}, \tag{1}$$

where T denotes the length of the sequence $r(t)$ and ν is the average firing rate. In stationary conditions and for sufficiently long T, Eq. (1) is equivalent to an averaging over the rate-determining signal ensemble, which removes the time dependence of the rate [1,7],

$$I_{\text{ind}} = \left\langle \frac{r(t)}{\nu} \log_2 \frac{r(t)}{\nu} \right\rangle_s, \tag{2}$$

with $\langle\rangle_s$ being the signal average.

The information per spike contained in entire spike trains of *correlated* spikes—here also referred to as "correlation method"—in its general form is given by [30]

$$I'_{\text{corr}} = -\frac{1}{2\nu}\int_{-\infty}^{\infty} df \log_2 \left(1 - \frac{C_{\text{cross}}(f)}{C_{\text{auto}}(f)}\right). \tag{3}$$

Here, $C_{\text{cross}}(f)$ and $C_{\text{auto}}(f)$ denote the Fourier transformed spike cross- and autocorrelation, respectively. Cross correlations are calculated between the spike trains that result from different presentations of the same stimulus, and autocorrelations are calculated for each spike train and averaged over different stimulus presentations (see Methods, Sec. III B). Notably, I'_{corr} is exact under the assumption of stationary signals and neurons with finite memory but does not require Gaussianity in the signal [30]. In Poisson neurons, spike correlations only emerge from signal-induced correlations in the rate trajectory (Fig. 1) and are equivalent to rate correlations. In this case, the Fourier transformed correlation functions can be expressed in terms of the mean firing rate ν and the rate power spectrum $S_{rr}(f)$ only (see Appendix B for details):

$$C_{\text{cross}}(f) = S_{rr}(f), \tag{4}$$

$$C_{\text{auto}}(f) = C_{\text{cross}}(f) + \nu. \tag{5}$$

This is consistent with the fact that the cross correlation is equivalent to the autocorrelation of the peristimulus time histogram (PSTH) [30] which in turn is given by $r(t)$. It follows that under the assumption of only signal-related spike correlations Eq. (3) can be written as

$$I_{\text{corr}} = -\frac{1}{2\nu}\int_{-\infty}^{\infty} df \log_2 \left(1 - \frac{S_{rr}(f)}{\nu + S_{rr}(f)}\right). \tag{6}$$

We note that Eq. (6) can be computed knowing only $r(t)$ and therefore does not require more knowledge than Eq. (1); both expressions can be determined in terms of the PSTH only (see Sec. III B), which corresponds to $r(t)$ and is experimentally accessible. Importantly, for non-Poisson neurons Eq. (6) can be considered an approximation of the mutual information when only rate correlations are taken into account and all other correlations (e.g., intrinsic or noise correlations) are neglected. Moreover, we would like to highlight that in the given framework the correlation method is equivalent to previously used lower and upper bound information estimates (see Appendix A).

The difference $I_{\text{ind}} - I_{\text{corr}}$ is the redundancy among spikes that arises from signal correlations in Poisson neurons, or generally from rate correlations as obtained from the PSTH. More generally, the difference $I_{\text{ind}} - I'_{\text{corr}}$ is the redundancy introduced by all present spike correlations and therefore offers a way to compute the difference in information if all but rate correlations are ignored.

B. Rate distribution only determines mutual information if correlations are neglected

Although the information for independent and correlated spikes can both be expressed as a function of the rate trajectory, it is different features of that trajectory that determine the information in either case. Considering independent spikes means neglecting all temporal spike correlations, both intrinsic and signal induced. Accordingly, I_{ind} does not contain any temporal correlations and is well determined by the distribution of $r(t)$ [cf. Eq. (2); we note that I_{ind} is invariant under any linear rescaling of $r(t)$ that leaves the ratio σ_r/ν unchanged]. On the other hand, I_{corr}—considering Poisson neurons with rate correlations—depends on the power spectrum of $r(t)$ [see Eq. (6)]. In the following, we elaborate on the differences between I_{ind} and I_{corr} by means of three example processes for the signal that are characterized in terms of their rate distribution and dynamics. All processes are assumed to be stationary and their dynamical properties are specified subsequently.

1. *Uniform rate distribution*

First, we consider a rate process with uniform distribution. Uniform rate distributions across stimuli have been argued to optimize encoding under certain circumstances [40,41]. At a given mean rate ν and standard deviation σ_r it follows from Eq. (2) that the information contained in single spikes generated by a uniform rate distribution is given by (cf. Methods, Sec. III C)

$$\begin{aligned} I_{\text{ind}}^{\text{uni}} &= \frac{1}{2\sigma_r\sqrt{3}}\int_{\nu-\sqrt{3}\sigma_r}^{\nu+\sqrt{3}\sigma_r} dr \frac{r}{\nu}\log_2\frac{r}{\nu} \\ &= \frac{-(\nu^2 + 3\sigma_r^2 - 2\sqrt{3}\nu\sigma_r)\ln\left(1 - \frac{\sqrt{3}\sigma_r}{\nu}\right)}{4\sqrt{3}\nu\sigma_r\ln(2)} \\ &\quad + \frac{(\nu^2 + 3\sigma_r^2 + 2\sqrt{3}\nu\sigma_r)\ln\left(\frac{\sqrt{3}\sigma_r}{\nu} + 1\right) - 2\sqrt{3}\nu\sigma_r}{4\sqrt{3}\nu\sigma_r\ln(2)}. \end{aligned} \tag{7}$$

2. *Telegraph process*

The second rate process we consider is the telegraph process. It is a binary process with states $\nu \pm \sigma_r$ and mean ν. Assuming equal probabilities for both states (see methods

Sec. III D) we find for the independent spike information

$$I_{\mathrm{ind}}^{\mathrm{tele}} = \frac{1}{2}\sum_{k=\{1,-1\}} \frac{\nu + k\sigma_r}{\nu}\log_2\frac{\nu + k\sigma_r}{\nu}. \tag{8}$$

3. Ornstein-Uhlenbeck process

Next, we consider rate trajectories that represent Ornstein-Uhlenbeck processes (OUPs) with mean ν and variance σ_r^2. The process has a Gaussian distribution (see Methods, Sec. III E) and it follows for the information contained in independent spikes:

$$I_{\mathrm{ind}}^{\mathrm{OU}} \approx \frac{1}{\sqrt{2\pi\sigma_r^2\nu^2}}\int_0^\infty dr\, \exp\left(\frac{-(r-\nu)^2}{2\sigma_r^2}\right) r\log_2\frac{r}{\nu}. \tag{9}$$

Here, the integration must be truncated to avoid negative firing rates. As a consequence, $I_{\mathrm{ind}}^{\mathrm{OU}}$ is an approximation which becomes more accurate for smaller σ_r/ν. Note that the generality of our results is not affected since all results are confirmed by and consistent with the analytic and exact results for the other processes.

According to Eq. (6), calculating the information in rate-correlated spikes requires knowledge of the rate power spectrum. The telegraph and Ornstein-Uhlenbeck process possess an exponentially decaying autocorrelation function (see method Sec. III F). Here we assign the same autocorrelation function to the process with uniform rate distribution for the purpose of demonstration. The power spectrum of a process with exponentially decaying autocorrelation reads

$$S_{rr}^{\mathrm{exp}}(f) = \frac{\sigma_r^2\tau}{\pi(1+f^2\tau^2)}, \tag{10}$$

where τ is the correlation time. From Eq. (6) follows that the information in correlated spikes at the given rate power spectrum is the same for all three processes,

$$I_{\mathrm{corr}}^{\mathrm{exp}} = I_{\mathrm{corr}}^{\mathrm{uni}} = I_{\mathrm{corr}}^{\mathrm{tele}} = I_{\mathrm{corr}}^{\mathrm{OU}}, \tag{11}$$

and reads

$$\begin{aligned} I_{\mathrm{corr}}^{\mathrm{exp}} &= -\frac{1}{2\nu}\int_{-\infty}^{\infty} df\, \log_2\left(1 - \frac{S_{rr}^{\mathrm{exp}}(f)}{\nu + S_{rr}^{\mathrm{exp}}(f)}\right) \\ &= \frac{\pi^{3/2}\nu - \pi\sqrt{\nu(\pi\nu + \sigma_r^2\tau)} + \sqrt{\pi}\sigma_r^2\tau}{\tau\ln(2)\sqrt{\nu^3(\pi\nu + \sigma_r^2\tau)}}. \end{aligned} \tag{12}$$

With the results Eq. (7), (8), and (12) at hand, we make some interesting observations. First, even though all processes have the same spectral decomposition and variance, the information in spikes that are assumed to be independent is different because the distributions of $r(t)$ are different (see Fig. 2). Accordingly, if the overall distribution of $r(t)$ is fixed but the correlation time is varied, I_{ind} remains unchanged for all processes. On the other hand, the information contained in correlated spikes at a given signal power spectrum does not depend on the distribution of $r(t)$.

As a general finding, in rate modulated Poisson neurons the inclusion of signal-induced spike correlations always diminishes the information contained in spike trains compared to when spikes are treated as independent (see Figs. 2 and 3). This redundancy among spikes has been proposed before [1].

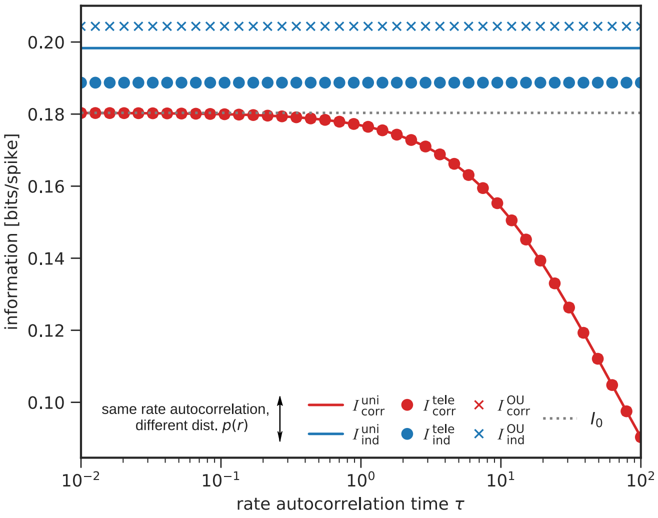

FIG. 2. Signal power spectrum determines the information contained in correlated spikes whereas the information in independent spikes is given through the signal distribution. The red (lower) line and symbols show the information of correlated spikes for a uniform, a telegraph, and an Ornstein-Uhlenbeck process, respectively. It is the same in all cases and varies with τ. On the other hand, the information contained in independent spikes [blue (upper) line and symbols] does not vary with τ but is different for all processes despite their identical spectra. Here, the differences in the probability distributions of $r(t)$ in the three processes lead to different encoding redundancies. The dashed line is the analytic limit $\lim_{\tau\to 0} I_{\mathrm{corr}} = I_0 = \frac{\sigma_r^2}{2\ln(2)\nu^2}$ [Eq. (19)]. For all curves it is $\nu = 1$ and $\sigma_r = 0.5\nu$.

C. At small rate modulations spikes are effectively independent irrespective of temporal correlation structure

As discussed above, correlated rate modulations diminish the transmitted information. We can expect the contribution of correlations to vanish in the limit $\sigma_r \to 0$. In the following we show how this limit leads to an equivalence of I_{ind} and I_{corr}.

Because $[r(t) - \nu] \to 0$ when $\sigma_r \to 0$, we can expand the integrand of Eq. (1) in $r(t)$ around ν. Expanding up to second order we get

$$I_{\mathrm{ind}} \approx \frac{1}{T}\int_0^T dt\, \frac{r(t)-\nu}{\nu\ln(2)} + \frac{[r(t)-\nu]^2}{2\nu^2\ln(2)} = \frac{\sigma_r^2}{2\ln(2)\nu^2}. \tag{13}$$

The first term of the integrand vanishes because the time average of $r(t)$ is ν, and the time average of the numerator of the second term is the rate variance. This result is consistent with first order expansions of Eqs. (7) and (8) in σ_r^2.

For the correlation method of Eq. (6) the limit $\sigma_r \to 0$ implies that we can expand I_{corr} in $S_{rr}(f)$ at each frequency. Expanding to first order in $S_{rr}(f)$ we obtain

$$I_{\mathrm{corr}} \approx \frac{1}{2\ln(2)\nu^2}\int_{-\infty}^{\infty} df\, S_{rr}(f) = \frac{\sigma_r^2}{2\ln(2)\nu^2}. \tag{14}$$

Thus, in the limit of vanishing rate modulations both information estimates are equivalent as they possess the same leading order expansion in σ_r which is given by

$$I_0 \equiv \frac{\sigma_r^2}{2\ln(2)\nu^2}. \tag{15}$$

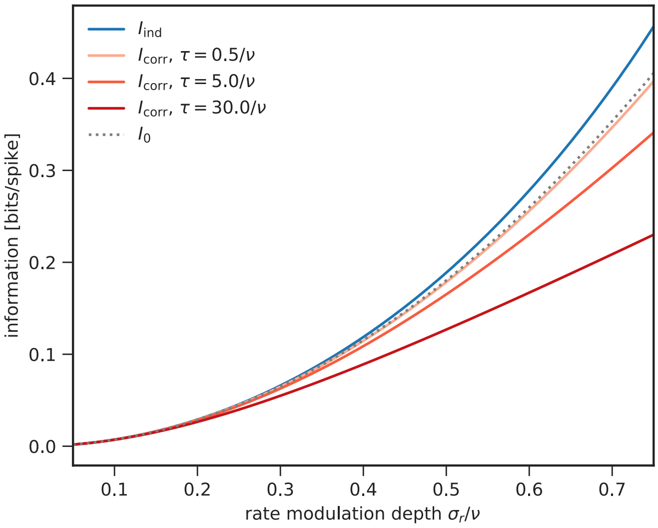

FIG. 3. Temporal correlations introduce redundancy. The information in independent spikes (upper curve) is always larger than that in correlated spikes (lower curves in shades of red). Shown here is the information per spike for telegraph processes with σ_r/ν as given on the x axis. In the limit of very small rate modulations ($\sigma_r \to 0$) both cases converge to I_0 [Eq. (15), shown as dashed line]. For all curves it is $\nu = 2$.

This result emphasizes that the information in both independent and correlated spikes are in leading order determined by the rate processes' variance that corresponds to the modulation depth or dynamic range around the baseline firing rate, irrespective of other statistical properties of $r(t)$.

D. Information in correlated spikes is maximized in the limit of vanishing correlation time

Intuitively, one way to reduce the impact of signal-induced rate correlations is to decrease the signal correlation time τ, because this reduces the width of the autocorrelation function. Here, we investigate the influence of vanishingly small correlation times on the information carried by correlated spikes.

A vanishing correlation time is equivalent to a flat signal power spectrum [cf. the power spectrum Eq. (10) as an example]. Therefore, we now consider a rate power spectrum $S_{rr}(f)$ that is constant for all frequencies $|f| \leqslant f_c$ and zero otherwise (e.g., band-limited white noise). Later we take the limit $f_c \to \infty$. For a given rate variance σ_r^2 it follows that

$$\int_{-f_c}^{f_c} df\, S_{rr}(f) = \sigma_r^2 \Rightarrow S_{rr}(f) = \sigma_r^2/(2f_c). \tag{16}$$

Inserting in Eq. (6) and expansion in $1/(2f_c)$ yields

$$I_{\mathrm{corr}} = -\frac{1}{2\nu}\int_{-f_c}^{f_c} df \log_2\left(1 - \frac{\sigma_r^2/(2f_c)}{\nu + \sigma_r^2/(2f_c)}\right) \tag{17}$$

$$= \frac{f_c}{\nu}\left\{\frac{\sigma_r^2/(2f_c)}{\nu \ln(2)} + \mathcal{O}\left[\left(\frac{\sigma_r^2}{2f_c}\right)^2\right]\right\}. \tag{18}$$

Now, the limit $\tau \to 0$ of vanishing correlation time corresponds to taking the limit $f_c \to \infty$ in the last equation. This limit exactly yields I_0 and hence it is

$$\lim_{\tau\to 0} I_{\mathrm{corr}} = I_0 \geqslant I_{\mathrm{ind}}. \tag{19}$$

This result is consistent with the limit $\tau \to 0$ of Eq. (12), representing the special case of an exponentially decaying autocorrelation function. In Figs. 2 and 3 the finding is illustrated by the fact that the curves of I_{corr} approach that of I_0 for decreasing correlation time. At a given rate variance I_0 serves as an upper bound for I_{corr}. However, we also know that I_0 is equivalent to the information in independent spikes only in the limit of vanishing rate modulations. Therefore, vanishing rate correlation times maximize the information in correlated spikes for an otherwise fixed rate process but do not generally coincide with the case where spikes carry information independently (cf. Fig. 2). From one perspective, this can be explained by the cumulative redundant effect of the spike correlations across frequencies, here captured by σ_r^2, which does not have to be small even if $S_{rr}(f)$ is small everywhere. Moreover, the result of Eq. (19) expresses an essential difference between the notions of independent spikes in I_{ind} and the zero correlation time limit of I_{corr}. The derivation of I_{ind} not only relies on the assumption of statistically independent firing rates at different times, but additionally assumes that the signal entropy is that of a homogeneous Poisson process [1,25,42] with rate ν an no rate modulations. The zero correlation time limit of I_{corr} on the other hand takes into account that rate modulations (with variance σ_r^2) are present, albeit independent across time.

III. METHODS

A. Poisson neurons

We consider spike trains which result from Poisson point processes with a dynamic rate $r(t)$. The spiking mechanisms can be described as follows: time is discretized in bins of size $\Delta \to 0$ that contain at most one spike [7,43]. In a given bin n at time $t_n = n\Delta$ a spike occurs with probability $p = \Delta r(t_n)$ no spike is emitted with probability $1 - p$. Spiking in a single bin hence occurs according to a Bernoulli process with probability p. Poisson spiking implies that all time bins are conditionally independent given the firing rate. In particular, the probability of spiking in one time bin is not conditioned on the probability of spiking in any other time bin [43]. Poisson neurons with a constant rate exhibit a coefficient of variation and Fano factor of 1 in their firing statistics [44]. They have been found to be an appropriate description for the noise characteristics and firing irregularity in biological neurons [33–35].

B. Spike correlation functions

We define the Fourier transform of a time series $g(t)$ with length T as

$$\mathcal{F}(g(t)) = \tilde{g}(f) = \int_0^T g(t)e^{-i2\pi ft}dt. \tag{20}$$

In this article we assume $T \to \infty$. The rate power spectrum is defined as the Fourier transformed autocorrelation of the rate trajectory $r(t)$,

$$S_{rr}(f) = |\tilde{r}(f)|^2, \tag{21}$$

where signal averaging is implicitly made because $T \to \infty$.

We represent spike trains $y(t)$ as sequences of δ peaks at spike times t_f, such that $y(t) = \sum_{t_f} \delta(t - t_f)$. Then, the autocorrelation function in frequency space is given by

$$C_{\text{auto}}(f) = \langle \tilde{y}_n(f) \tilde{y}_n^*(f) \rangle_{\text{tr}_n}, \tag{22}$$

where $\tilde{y}_n(f)$ is the Fourier transform of the spike train in trial n. For each trial $1, \ldots, N$ a new signal (here, rate trajectory) from the according stochastic ensemble is presented and averaging $\langle\rangle_{\text{tr}_n}$ occurs over all trials. One noteworthy property of C_{auto} is that its large frequency limit is equal to the average firing rate, $\lim_{f\to\infty} C_{\text{auto}}(f) = \nu$. The spike cross-correlation function is defined analogously as

$$C_{\text{cross}}(f) = \langle \tilde{y}_m(f) \tilde{y}_k^*(f) \rangle_{\text{tr}_{m\neq k}}. \tag{23}$$

Here, the averaging occurs over pairs of neurons or trials m and k whose spike trains originate from presentation of the same signal or rate.

C. Process with uniform distribution

If the rate process is assumed to follow a uniform distribution with a given mean ν and variance σ_r^2, the stationary probability for a rate r is given by

$$p(r) = \begin{cases} \frac{1}{2\sigma_r\sqrt{3}} & \text{if } -\sigma_r\sqrt{3} \leqslant r - \nu \leqslant \sigma_r\sqrt{3}, \\ 0 & \text{otherwise.} \end{cases} \tag{24}$$

This imposes a constraint on the maximum variance at a given mean rate in order to prevent overmodulation and mathematical inconsistencies; we require $\sigma_r \leqslant \nu/\sqrt{3}$.

D. Telegraph process

Another stochastic process we consider is the telegraph process, also called random telegraph noise. This process is a binary process that can assume the values $\nu + \sigma_r$ and $\nu - \sigma_r$. Jumping between these two processes occurs randomly with a specified rate that determines the correlation time of the process [45]. The telegraph process resembles the switching between up and down states of cortical activity [46–48]. Here, we assume that both values occur with equal probability. Hence,

$$p(r = \nu + \sigma_r) = p(r = \nu - \sigma_r) = 1/2. \tag{25}$$

To avoid negative rates, $\sigma_r \leqslant \nu$ is required.

E. Ornstein-Uhlenbeck process

Ornstein-Uhlenbeck processes (OUPs), also known as colored noise, are bandpass filtered versions of Gaussian white noise and have been found to be a good description of neuronal activity [49–51]. For rates following an OUP with mean ν and variance σ_r^2 the stationary probability distribution is given by a normal distribution,

$$p(r) = \mathcal{N}\big(r \big| \nu, \sigma_r^2\big). \tag{26}$$

Importantly, this normal distribution does not bound r and technically involves negative rates. In Results, Sec. II, the integration over $p(r)$ is restricted to non-negative rates, resulting in approximations to the mutual information (cf. Sec. II B 3).

At the same mean and variance, the uniform, telegraph, and Ornstein-Uhlenbeck processes realize fundamentally different rate distributions.

F. Exponentially decaying autocorrelation

Generally, the probability distribution of a stochastic process is—apart from mean and variance—independent of its autocorrelation function. In fact, stochastic processes with arbitrary probability distribution and autocorrelation can be generated [52,53]. An important class of stochastic processes are those with exponentially decaying autocorrelations. For example, Ornstein-Uhlenbeck processes, also known as colored noise, are characterized by this type of autocorrelation and have been found to be a good description of neuronal activity [49–51]. For a (signal-dependent) rate process $r(t)$ such a correlation reads

$$\frac{1}{T}\int_0^T dt\ r(t) r(t-h) - \nu^2 = \sigma_r^2\, e^{-|h|/\tau}, \tag{27}$$

where σ_r^2 and τ are the variance and correlation time, respectively. The corresponding power spectrum is given by Eq. (10). Telegraph and Ornstein-Uhlenbeck processes naturally have exponentially decaying autocorrelations [45]. This assumption is also made for the process with uniform distribution in order to completely specify its dynamical properties.

IV. RELATION TO PREVIOUS WORK

A number of studies has addressed the issue of redundancy in spikes both within and across cells (see, e.g., [24,27,28,54,55] or [6,29] for reviews). Here, we review these studies and relate them to our present work. We thereby focus on spike correlations in one neuron across time rather than across neurons.

Many previous studies have devised approximate expansions of the mutual information around I_{ind} [Eq. (2)], incorporating the effect of signal and noise correlations in higher order corrections to this expression. Such expansions of the mutual information were for example done in terms of the recording length for both spike count and rate codes [24] and temporal codes [27,54]. The result is a systematic decomposition of the mutual information in parts containing different types of signal and noise cross and autocorrelations. Investigating these components, the method allows us to identify whether the different correlations add synergy or redundancy to the neural code. Interestingly, if Poisson spiking is assumed, the only remaining correction to the information is given in terms of signal correlations and always reduces the overall information rendering Eq. (2) an upper bound, in accordance with our results (see, e.g., Sec. II D). The second order decomposition of the information has been proven a good approximation for short windows of stimulus presentation and low firing rates [27] (effectively, correlations between more than two spikes are assumed to be negligible for information transmission [6]). Our study, on the other hand, assumes recording windows that are much longer than the signal correlation time and that contain many spikes; in this setting our results are exact.

An expansion similar to [54] has been put forward by DeWeese [25,42] for single cells only and comprises a cluster expansion in the signal correlation time around Eq. (2). This yields similar results as [54] and [27] but omits terms that contain spike correlations at equal times [27,42]. Taking the limit of zero correlation time in this expansion only leaves the leading order term I_{ind}. This, however, is only an upper bound for the same limit of the correlation method Eq. (6). Again, we argue that this discrepancy reflects the different assumptions about the signal averaged spiking statistics in the two methods [Eq. (1) vs Eq. (6)]. In one case the zeroth order expansion of the signal entropy is that of a homogeneous Poisson process (with the signal-averaged firing rate) and hence oblivious of rate modulations. The correlation method takes these modulations into account and depends on the variance of the rate process [cf. Eq. (19)]. Rate modulations thus contribute to the information even if they are independent across time. Therefore, both methods provide different reference values for the information in independent spikes depending on the moments of the stationary rate distribution that are considered relevant. Often the effect of correlations is measured by means of a reference that is computed on shuffled spiking data [6,29]. Shuffling a modulated rate process in time leaves both mean and variance unchanged. We therefore think the limit I_0 serves as a good alternative reference for the information in independent spikes and could be used as such in future studies.

An exact decomposition of the mutual information has been put forward by Pola *et al.* [28] and enables the investigation of synergy and redundancy among spikes, including all effects of correlations within and across cells. Similar to [27,54], the information is decomposed in a linear term, a signal-similarity term, a stimulus-independent correlational component, and a stimulus-dependent correlational component [28] (a similar decomposition of the population information is presented in [6]). This method thereby generally allows for an exact and rigorous investigation of the effects of different kinds of correlations on information transmission. In particular, the role of cross-neural correlations that are not investigated here can be addressed with this method. However, the decomposition method does not explicitly provide a means to determine the effect of temporal spike correlations on information transmission. In fact, considering single neurons the only remaining term in the method of [28] is I_{lin} and merely describes the information in single neurons in most general terms as mutual information of signal and spiking response.

Because the method of [28] is based on computing probability distributions over all possible spike trains it is in practice limited by the analytical tractability of these probabilities and encounters problems with sampling biases for experimental data of limited size [6,28,55]. Other studies addressed this problem and introduced shuffling methods to reduce the bias in lower and upper bounds to the information [55,56]. Their approach comprises an estimation of the role of correlations for information transmission in terms of general response distributions that had previously been proposed [57,58] (and whose validity has been debated [6,29]). However, due to the "curse of dimensionality" these methods cannot overcome the sampling problem when, e.g., large sequences with high temporal resolution are considered.

The correlation method of the present study only requires pairwise spike correlations and hence requires only knowledge of the second order statistics of the spiking responses. These properties are well accessible both analytically and experimentally. This renders Eqs. (2), (3), and (6) convenient tools for the investigation of the role of spike correlations in cases where long, stationary stimuli with finite correlation time can be assumed. In situations where short recording lengths, low spike counts, or very slow signals are present, or when cross-neural correlations are considered, other methods discussed in this section are more appropriate (see, e.g., [14,57,59] for applications on real data).

V. SUMMARY AND GENERAL DISCUSSION

In this study we analyzed the information content and encoding redundancy that stems from temporal (signal-induced) rate correlations. Deriving the information contained in an inhomogeneous Poisson point process which encodes a continuous valued signal by modulation of the firing rate, we showed that the information in neurons with only rate correlations can be expressed using second-order statistics of the PSTH only [Eq. (6)]. Contrasting this to the information carried by neurons that are considered independent, we could analytically determine the amount of redundantly encoded information due to temporal correlations. With this approach we confirmed that growing rate correlation amplitudes increase the encoding redundancy among spikes (see Fig. 3) [1]. We illustrated that the information in independent and rate-correlated spikes is completely determined by first-order (overall distribution) and second-order (autocorrelation) statistics of the rate trajectory, respectively. As a rather surprising consequence the information in rate modulated Poisson neurons only depends on the spikes' autocorrelation structure, regardless of other properties of the rate trajectory (see Fig. 2).

Moreover, we mathematically proved the intuition that the information in correlated and independent spikes becomes identical in the limit of vanishing rate modulations. We further demonstrated that signals with a vanishing correlation time (a flat spectrum) maximize the information in correlated spikes, but do not generally lead to independent spikes even in Poisson neurons. Importantly, our results are not restricted to Gaussian rate processes and we showed that a given signal power spectrum can be realized through different (non-Gaussian) processes [60] which yield different redundancy.

From our results follows that it may be beneficial for a neural system to temporally decorrelate either its input statistics, or intrinsically decorrelate the response to a correlated input. This could be done by low signal-dependent rate modulation depths. However, this at the same time reduces the overall information transmission. As follows from Figs. 2 and 3, a better strategy would be to minimize the correlation time in order to maximize information transmission. This is known as temporal whitening and can be implemented, e.g., through fast synapses or adaptation mechanisms [5,61–65]. One of our findings is that even complete whitening does not lift the information to the level of genuinely independent spikes as characterized by I_{ind} (cf. Sec. IV). Whereas previous theoretical and experimental studies have shown that neurons can transmit information independently [43,57,66], it seems to be unclear whether whitening of the neural responses also implies independent spikes as is often assumed [5,43]. However, these remaining levels of redundancy after whitening may be beneficial and increase the robustness to noise by providing longer windows for reliable signal integration. This is particularly true if external (input) noise sources are relevant. In our model framework all noise effects are summarized in the Poisson spiking variability (Fano factor of 1) and noise sources cannot be separated.

In Sec. II C we showed that there is a mathematical limit at which the information for independent spikes and the correlation method converge to an expression I_0 that only depends on the dynamic range of the rate trajectory. Whereas this appears to be an intuitive result it has not been formally obvious because I_{corr} and I_{ind} have been formulated in the time and frequency domain, respectively. The finding links previous work on the Poisson limit [1], lower and upper bound calculations [31], and the more recent analysis of the complete mutual information [30]. At the same time it provides a very intuitive notion for the information transmission in a rate code at lowest order: information is proportional to the squared coefficient of variation of the rate process. This in turn is in accordance with the view that the quality of a rate code grows with its dynamic range—as long as approximately linear signal-rate relations hold.

In order to derive I_{corr} [Eq. (6)] we make the assumption of Poisson firing which has been proven to be reasonable in many cases for cortical neurons but cannot be considered to be always valid [32,67]. The present work focuses on the impact of external signals whose correlations are reflected in rate correlations. Nonetheless, I_{corr} can be computed for any spiking data irrespective of their correlation structure, e.g., obtained from simulations, recorded data or analytical calculations, as long as stationarity criteria are fulfilled [1,30]. It then corresponds to the information carried by the rate modulation only, ignoring other correlations and temporal codes with high temporal precision. It can be used to distinguish the effects of rate correlations and other correlations, such as intrinsic noise correlations, by comparing I'_{corr} to I_{ind}.

In a linear rate encoding [$r(t) \sim s(t)$], signal correlations and rate correlations are equivalent (cf Fig. 1). However, in neural circuits stimulus changes are not generally translated into proportional rate changes, and signal and rate correlations are not necessarily equivalent [43]. Often, linear approximations of the input-output relations are appropriate [68] and can be obtained analytically for neuron models [69–71], and then $I_{\mathrm{ind}} - I_{\mathrm{corr}}$ measures the effect of signal-induced correlations only. If the assumptions of rate encoding and linearity are not given $I_{\mathrm{ind}} - I'_{\mathrm{corr}}$ can be used to determine the role of other correlations, such as higher-order rate correlations [20] and intrinsic correlations [44]. We have restricted our analysis to signal-induced rate correlations in order to introduce a general, analytic framework. However, this could certainly be an important focus for future experimental and theoretical studies. Applying our approach to *in vivo* data by calculating the respective first and second order spiking statistics could help shed light on the controversial role of spiking correlations for neural coding.

Neurons are embedded in networks in which interneural correlations can arise [72], even though these correlations are considered to vanish in balanced networks [73]. In particular, noise correlations can generally have additional synergetic or redundant effects on population encoding (see [74,75] for reviews). In this work signal correlations are incorporated through the signal-carrying rate trajectories; noise correlations are not present in the Poisson framework but have been found to be small [76]. Moreover, because our work represents the limit of disconnected neurons it can promote network level studies by providing a reference for redundancy effects that are not mediated by interneural coupling but by temporal interactions only. Future extensions of the present work to population encoding could be guided by previous studies that include cross-neural noise and signal correlations [6,27,28,54,58] (see Sec. IV).

In summary, our work provides analytically and experimentally accessible methods to compute the influence of rate correlations on redundancy in neural information encoding. These influences are reducible to simple first and second order statistics of the rate process. Comparing our results to existing results reconciles different methodologies that have been present in the field.

ACKNOWLEDGMENTS

This work has been supported by the Max Planck Society, the DFG via CRC1080, and the Polytechnische Gesellschaft (T.T.) T.H. acknowledges the travel support of the Joachim Herz Foundation.

APPENDIX A: COMPARISON TO BOUNDED INFORMATION ESTIMATIONS

Here, we show that the complete mutual information I'_{corr} from Eq. (3) is indeed equivalent to the previously used lower and upper bounds for the information for rate modulated Poisson neurons.

1. Lower bound estimation

A commonly used method to determine the information (per spike) in spike trains is given by the information content that can be decoded linearly. In its general form it is given by [31,77]

$$I_{\mathrm{ld}} = -\frac{1}{2\nu}\int_{-\infty}^{\infty} df \log_2\left(1 - \frac{|S_{sy}(f)|^2}{S_{ss}(f)C_{\mathrm{auto}}(f)}\right), \tag{A1}$$

where $S_{sy}(f)$ is the cross spectrum of signal $s(t)$ and spiking responses $y(t)$, defined by

$$S_{sy}(f) = \lim_{T\to\infty}\langle \tilde{s}(f)\tilde{y}^*(f)\rangle_T, \tag{A2}$$

and $S_{ss}(f)$ is the signal autocorrelation. This information estimate has been used in numerous studies [65,78–83] and represents a *lower bound* for the total information content [31]. It is obtained as the mutual information of the signal and a response based linear signal reconstruction. Nonlinear signal-response correlations cannot be captured by Eq. (A1) and are equivalent to noise from the information transmission perspective.

As described in Methods, Sec. III B, if the signal is equivalent to $r(t)$ it is $S_{sy}(f) = S_{rr}(f) = C_{\mathrm{cross}}(f)$ [see Eq. (B9) below]. Inserting these relations in Eq. (A1) reveals that the linearly decodable information is equivalent to the full information Eq. (3). This is an intuitive finding since by design the signal is linearly encoded in the firing rate such that all information is linearly encoded in rate modulations.

2. Upper bound estimation

An upper bound for the mutual information as introduced previously [31,84,85] is given by

$$I_{ub} = -\frac{1}{2}\int_{-\infty}^{\infty} df \log_2\left[1-\gamma_{y_1y_2}(f)\right]df, \tag{A3}$$

where

$$\gamma^2_{y_1y_2} = \lim_{T\to\infty}\frac{|\langle\tilde{y}_1(f)\tilde{y}_2^*(f)\rangle|^2}{|\langle\tilde{y}_1(f)\rangle|^2|\langle\tilde{y}_2(f)\rangle|^2}, \tag{A4}$$

with spiking responses y_1, y_2 to the same signal at different trials. We identify $|\langle\tilde{y}_1(f)\tilde{y}_2^*(f)\rangle| = C_{\text{cross}}(f)$ and $|\langle\tilde{y}_1(f)\rangle|^2 = |\langle\tilde{y}_2(f)\rangle|^2 = C_{\text{auto}}(f)$ using standard stationarity assumptions and the relations from Methods, Sec. III B. Given these identities, we recognize that the upper bound Eq. (A3) and exact information Eq. (3) are equivalent. Importantly, this is the case irrespective of the Poisson spiking assumption.

APPENDIX B: SPIKE CORRELATION FUNCTIONS FOR POISSON NEURONS

In this section we illustrate in some more detail how the correlation functions Eqs. (4) and (5) can be derived from the properties of Poisson spike generation.

In the time domain the cross-correlation function of two spike trains from trials m and k at time lag h, generated through a Poisson process (see Sec. III A) with rate $r(t)$, is given by

$$\mathcal{F}^{-1}\{C_{\text{cross}}(f)\}(h) = \frac{1}{T}\int_0^T dt\ \langle y_m(t)y_k(t-h)\rangle_{\text{tr}_{m\neq k}}, \tag{B1}$$

with trial average $\langle\rangle_{\text{tr}}$. As the probabilities of spiking are conditionally independent between trials it follows that

$$\begin{aligned}\mathcal{F}^{-1}\{C_{\text{cross}}(f)\}(h) &= \frac{1}{T}\int_0^T dt\ \langle y_m(t)\rangle_{\text{tr}_m}\langle y_k(t-h)\rangle_{\text{tr}_k} & \text{(B2)}\\ &= \frac{1}{T}\int_0^T dt\ r(t)r(t-h). & \text{(B3)}\end{aligned}$$

Here, $r(t) = \langle y(t)\rangle$ is the definition of the rate in the sense of a PSTH. Fourier transforming Eq. (B3) yields Eq. (5) and is equivalent to the (Fourier transformed) autocorrelation of the PSTH (cf. [30]).

Similarly, the autocorrelation function in the time domain is given by

$$\mathcal{F}^{-1}\{C_{\text{auto}}(f)\}(h) = \frac{1}{T}\int_0^T dt\,\langle y_m(t)y_m(t-h)\rangle_{\text{tr}_m}. \tag{B4}$$

Poisson spiking implies that the probability of spiking at time t only depends on $r(t)$ (by independence) and therefore at any lag $|h| > 0$ different and equal trials are not distinguishable. Consequently, for finite lag the trial average in the previous equation again factorizes. Hence, for $|h| > 0$ it is $\mathcal{F}^{-1}\{C_{\text{auto}}(f)\}(h) = \mathcal{F}^{-1}\{C_{\text{cross}}(f)\}(h)$. For $h = 0$ the autocorrelation reads

$$\mathcal{F}^{-1}\{C_{\text{auto}}(f)\}(0) = \frac{1}{T}\int_0^T dt\ \left\langle y_m^2(t)\right\rangle_{\text{tr}_m}. \tag{B5}$$

Here, the integrand represents for each t the spike autocorrelation at zero time lag for a homogeneous Poisson process with rate $r(t)$. This holds even though time averaging is not carried out, because an averaging over a large (infinite) number of trials is equivalent. The autocorrelation of a homogeneous Poisson process is known [43]. Inserting and integrating over all times yields

$$\begin{aligned}\mathcal{F}^{-1}\{C_{\text{auto}}(f)\}(0) &= \frac{1}{T}\int_0^T dt\ r(t)\delta(0) + r^2(t) & \text{(B6)}\\ &= \nu\delta(0) + \sigma_r^2 + \nu^2. & \text{(B7)}\end{aligned}$$

Here, the last two terms are negligible as they are much smaller than $\nu\delta(0)$ and only present at $h = 0$, and therefore do not contribute to the Fourier transform yielding $C_{\text{auto}}(f)$ as $T\to\infty$. Taken together, the autocorrelation in the time domain hence reads

$$\mathcal{F}^{-1}\{C_{\text{auto}}(f)\}(h) = \nu\delta(h) + \frac{1}{T}\int_0^T dt\ r(t)r(t-h), \tag{B8}$$

and Eq. (4) can be obtained as its Fourier transform.

Using similar arguments as above we also find that

$$\frac{1}{T}\int_0^T dt\ \langle y_m(t)r_m(t-h)\rangle_{\text{tr}_m} = \frac{1}{T}\int_0^T dt\ r(t)r(t-h), \tag{B9}$$

because the rate is fixed across trials (with the same signal) and we assumed $r(t)\sim s(t)$. Therefore, here the signal-response cross correlation is equivalent to the spike autocorrelation. We made use of this relation in Appendix A 1.

---

[1] N. Brenner, S. P. Strong, R. Koberle, W. Bialek, and R. R. de Ruyter van Steveninck, Synergy in a neural code, Neural Comput. **12**, 1531 (2000).

[2] H. B. Barlow, Possible principles underlying the transformations of sensory messages, in *Sensory Communication*, edited by W. A. Rosenblith (John Wiley and Sons, New York, 1961), Chap. 13, pp. 217–234.

[3] J. J. Atick, Could information theory provide an ecological theory of sensory processing? Netw., Comput. Neural Syst. **3**, 213 (1992).

[4] M. J. Wainwright, Visual adaptation as optimal information transmission, Vision Res. **39**, 3960 (1999).

[5] F. Rieke, *Spikes: Exploring the Neural Code* (MIT, Cambridge, MA, 1999).

[6] E. Schneidman, W. Bialek, and M. J. Berry, Synergy, redundancy, and independence in population codes, J. Neurosci. **23**, 11539 (2003).

[7] A. Fairhall, Spike coding, in *Bayesian Brain: Probabilistic Approaches to Neural Coding*, edited by K. Doya (MIT, Cambridge, MA, 2007), p. 17.

[8] W. E. Skaggs, B. L. McNaughton, K. M. Gothard, and E. J. Markus, An information-theoretic approach to deciphering the hippocampal code, in *Advances in Neural Information Processing Systems 5*, edited by S. J. Hanson, J. D. Cowan,

and C. L. Giles (Morgan-Kaufmann, Burlington, MA, 1993), pp. 1030–1037.

[9] E. J. Markus, C. A. Barnes, B. L. McNaughton, V. L. Gladden, and W. E. Skaggs, Spatial information content and reliability of hippocampal CA1 neurons: effects of visual input, Hippocampus **4**, 410 (1994).

[10] W. E. Skaggs, B. L. McNaughton, M. A. Wilson, and C. A. Barnes, Theta phase precession in hippocampal neuronal populations and the compression of temporal sequences, Hippocampus **6**, 149 (1996).

[11] B. C. Souza, R. Pavao, H. Belchior, and A. B. L. Tort, On information metrics for spatial coding, Neuroscience **375**, 62 (2018).

[12] K. Mizuseki and G. Buzsáki, Preconfigured, skewed distribution of firing rates in the hippocampus and entorhinal cortex, Cell Rep. **4**, 1010 (2013).

[13] E. T. Rolls, A. Treves, M. J. Tovee, and S. Panzeri, Information in the neuronal representation of individual stimuli in the primate temporal visual cortex, J. Comput. Neurosci. **4**, 309 (1997).

[14] S. Panzeri, R. S. Petersen, S. R. Schultz, M. Lebedev, and M. E. Diamond, The role of spike timing in the coding of stimulus location in rat somatosensory cortex, Neuron **29**, 769 (2001).

[15] J. Gjorgjieva, H. Sompolinsky, and M. Meister, Benefits of pathway splitting in sensory coding, J. Neurosci. **34**, 12127 (2014).

[16] A. Kruscha and B. Lindner, Spike-count distribution in a neuronal population under weak common stimulation, Phys. Rev. E **92**, 052817 (2015).

[17] K. Hardcastle, N. Maheswaranathan, S. Ganguli, and L. M. Giocomo, A multiplexed, heterogeneous, and adaptive code for navigation in medial entorhinal cortex, Neuron **94**, 375 (2017).

[18] S. M. Chase and E. D. Young, First-spike latency information in single neurons increases when referenced to population onset, Proc. Natl. Acad. Sci. USA **104**, 5175 (2007).

[19] T. Gollisch and M. Meister, Rapid neural coding in the retina with relative spike latencies, Science **319**, 1108 (2008).

[20] S. O. Voronenko and B. Lindner, Weakly nonlinear response of noisy neurons, New J. Phys. **19**, 033038 (2017).

[21] S. P. Strong, R. Koberle, R. R. de Ruyter van Steveninck, and W. Bialek, Entropy and Information in Neural Spike Trains, Phys. Rev. Lett. **80**, 197 (1998).

[22] P. Reinagel and R. C. Reid, Temporal coding of visual information in the thalamus, J. Neurosci. **20**, 5392 (2000).

[23] S. Panzeri and A. Treves, Analytical estimates of limited sampling biases in different information measures, Netw., Comput. Neural Syst. **7**, 87 (1996).

[24] S. Panzeri, S. R. Schultz, A. Treves, and E. T. Rolls, Correlations and the encoding of information in the nervous system, Proc. Biol. Sci. **266**, 1001 (1999).

[25] M. DeWeese, Optimization principles for the neural code, in *Advances in Neural Information Processing Systems 8*, edited by D. S. Touretzky, M. C. Mozer, and M. E. Hasselmo (MIT Press, Cambridge, MA, 1996), pp. 281–287.

[26] R. S. Petersen, S. Panzeri, and M. E. Diamond, Population coding of stimulus location in rat somatosensory cortex, Neuron **32**, 503 (2001).

[27] S. Panzeri and S. R. Schultz, A unified approach to the study of temporal, correlational, and rate coding, Neural Comput. **13**, 1311 (2001).

[28] G. Pola, A. Thiele, K. P. Hoffmann, and S. Panzeri, An exact method to quantify the information transmitted by different mechanisms of correlational coding, Netw., Comput. Neural Syst. **14**, 35 (2003).

[29] P. E. Latham and S. Nirenberg, Synergy, redundancy, and independence in population codes, revisited, J. Neurosci. **25**, 5195 (2005).

[30] A. Dettner, S. Münzberg, and T. Tchumatchenko, Temporal pairwise spike correlations fully capture single-neuron information, Nat. Commun. **7**, 13805 (2016).

[31] A. Borst and F. E. Theunissen, Information theory and neural coding, Nat. Neurosci. **2**, 947 (1999).

[32] W. R. Softky and C. Koch, The highly irregular firing of cortical cells is inconsistent with temporal integration of random EPSPs, J. Neurosci. **13**, 334 (1993).

[33] M. N. Shadlen, K. H. Britten, W. T. Newsome, and J. A. Movshon, A computational analysis of the relationship between neuronal and behavioral responses to visual motion, J. Neurosci. **16**, 1486 (1996).

[34] D. J. Tolhurst, J. A. Movshon, and A. F. Dean, The statistical reliability of signals in single neurons in cat and monkey visual cortex, Vision Res. **23**, 775 (1983).

[35] E. D. Gershon, M. C. Wiener, P. E. Latham, and B. J. Richmond, Coding strategies in monkey v1 and inferior temporal cortices, J. Neurophysiol. **79**, 1135 (1998).

[36] W. J. Ma, J. M. Beck, P. E. Latham, and A. Pouget, Bayesian inference with probabilistic population codes, Nat. Neurosci. **9**, 1432 (2006).

[37] M. E. Mazurek and M. N. Shadlen, Limits to the temporal fidelity of cortical spike rate signals, Nat. Neurosci. **5**, 463 (2002).

[38] A. Compte, C. Constantinidis, J. Tegnér, S. Raghavachari, M. V. Chafee, P. S. Goldman-Rakic, and X.-J. Wang, Temporally irregular mnemonic persistent activity in prefrontal neurons of monkeys during a delayed response task, J. Neurophysiol. **90**, 3441 (2003).

[39] C. Geisler, N. Brunel, and X.-J. Wang, Contributions of intrinsic membrane dynamics to fast network oscillations with irregular neuronal discharges, J. Neurophysiol. **94**, 4344 (2005).

[40] M. Stemmler and C. Koch, How voltage-dependent conductances can adapt to maximize the information encoded by neuronal firing rate, Nat. Neurosci. **2**, 521 (1999).

[41] L. F. Abbott and S. X. Luo, A step toward optimal coding in olfaction, Nat. Neurosci. **10**, 1342 (2007).

[42] M. R. DeWeese, Optimization principles for the neural code, Ph.D. thesis, Princeton University, 1995.

[43] P. Dayan and L. F. Abbott, *Theoretical Neuroscience* (MIT, Cambridge, MA, 2001), Vol. 806.

[44] W. Gerstner and W. M. Kistler, *Spiking Neuron Models: Single Neurons, Populations, Plasticity* (Cambridge University Press, Cambridge, UK, 2002).

[45] K. Jacobs, *Stochastic Processes for Physicists: Understanding Noisy Systems* (Cambridge University Press, Cambridge, UK, 2010).

[46] T. A. Engel, N. A. Steinmetz, M. A. Gieselmann, A. Thiele, T. Moore, and K. Boahen, Selective modulation of cortical state during spatial attention, Science **354**, 1140 (2016).

[47] Y. Shu, A. Hasenstaub, and D. A. McCormick, Turning on and off recurrent balanced cortical activity, Nature (London) **423**, 288 (2003).

[48] G. Deco, D. Martí, A. Ledberg, R. Reig, and M. V. S. Vives, Effective reduced diffusion-models: a data driven approach to the analysis of neuronal dynamics, PLoS Comput. Biol. **5**, e1000587 (2009).

[49] D. T. Gillespie, Exact numerical simulation of the Ornstein-Uhlenbeck process and its integral, Phys. Rev. E **54**, 2084 (1996).

[50] A. Destexhe, M. Rudolph, and D. Paré, The high-conductance state of neocortical neurons in vivo, Nat. Rev. Neurosci. **4**, 739 (2003).

[51] A. Rauch, G. La Camera, H.-R. Lüscher, W. Senn, and S. Fusi, Neocortical pyramidal cells respond as integrate-and-fire neurons to in vivo–like input currents, J. Neurophysiol. **90**, 1598 (2003).

[52] S. Primak, V. Lyandres, and V. Kontorovich, Markov models of non-gaussian exponentially correlated processes and their applications, Phys. Rev. E **63**, 061103 (2001).

[53] I. W. Hunter and R. E. Kearney, Generation of random sequences with jointly specified probability density and autocorrelation functions, Biol. Cybern. **47**, 141 (1983).

[54] S. R. Schultz and S. Panzeri, Temporal Correlations and Neural Spike Train Entropy, Phys. Rev. Lett. **86**, 5823 (2001).

[55] M. A. Montemurro, R. Senatore, and S. Panzeri, Tight data-robust bounds to mutual information combining shuffling and model selection techniques, Neural Comput. **19**, 2913 (2007).

[56] G. Pola, R. S. Petersen, A. Thiele, M. P. Young, and S. Panzeri, Data-robust tight lower bounds to the information carried by spike times of a neuronal population, Neural Comput. **17**, 1962 (2005).

[57] S. Nirenberg, S. M. Carcieri, A. L. Jacobs, and P. E. Latham, Retinal ganglion cells act largely as independent encoders, Nature (London) **411**, 698 (2001).

[58] S. Nirenberg and P. E. Latham, Decoding neuronal spike trains: How important are correlations? Proc. Natl. Acad. Sci. USA **100**, 7348 (2003).

[59] C. Kayser, M. A. Montemurro, N. K. Logothetis, and S. Panzeri, Spike-phase coding boosts and stabilizes information carried by spatial and temporal spike patterns, Neuron **61**, 597 (2009).

[60] G. M. Jenkins and D. G. Watts, *Spectral Analysis and its Applications* (Oakland: Holden-Day, 1968).

[61] X.-J. Wang, Y. Liu, M. V. Sanchez-Vives, and D. A. McCormick, Adaptation and temporal decorrelation by single neurons in the primary visual cortex, J. Neurophysiol. **89**, 3279 (2003).

[62] M. S. Goldman, P. Maldonado, and L. F. Abbott, Redundancy reduction and sustained firing with stochastic depressing synapses, J. Neurosci. **22**, 584 (2002).

[63] N. Spruston, P. Jonas, and B. Sakmann, Dendritic glutamate receptor channels in rat hippocampal CA3 and CA1 pyramidal neurons, J. Physiol. **482**, 325 (1995).

[64] N. Fourcaud and N. Brunel, Dynamics of the firing probability of noisy integrate-and-fire neurons, Neural Comput. **14**, 2057 (2002).

[65] C. Pozzorini, R. Naud, S. Mensi, and W. Gerstner, Temporal whitening by power-law adaptation in neocortical neurons, Nat. Neurosci. **16**, 942 (2013).

[66] T. J. Gawne, T. W. Kjaer, J. A. Hertz, and B. J. Richmond, Adjacent visual cortical complex cells share about 20% of their stimulus-related information, Cereb. Cortex **6**, 482 (1996).

[67] G. Maimon and J. A. Assad, Beyond poisson: increased spike-time regularity across primate parietal cortex, Neuron **62**, 426 (2009).

[68] T. Herfurth and T. Tchumatchenko, How linear response shaped models of neural circuits and the quest for alternatives, Curr. Opin. Neurobiol. **46**, 234 (2017).

[69] B. Lindner, L. Schimansky-Geier, and A. Longtin, Maximizing spike train coherence or incoherence in the leaky integrate-and-fire model, Phys. Rev. E **66**, 031916 (2002).

[70] M. J. E. Richardson, Firing-rate response of linear and nonlinear integrate-and-fire neurons to modulated current-based and conductance-based synaptic drive, Phys. Rev. E **76**, 021919 (2007).

[71] N. Brunel, F. S. Chance, N. Fourcaud, and L. F. Abbott, Effects of Synaptic Noise and Filtering on the Frequency Response of Spiking Neurons, Phys. Rev. Lett. **86**, 2186 (2001).

[72] A. Kohn, R. Coen-Cagli, I. Kanitscheider, and A. Pouget, Correlations and Neuronal Population Information, Annu. Rev. Neurosci. **39**, 237 (2016).

[73] C. van Vreeswijk and H. Sompolinsky, Chaos in neuronal networks with balanced excitatory and inhibitory activity, Science **274** 1724, (1996).

[74] B. B. Averbeck, P. E. Latham, and A. Pouget, Neural correlations, population coding and computation, Nat. Rev. Neurosci. **7**, 358 (2006).

[75] M. Shamir, Emerging principles of population coding: in search for the neural code, Curr. Opin. Neurobiol. **25**, 140 (2014).

[76] M. R. Cohen and A. Kohn, Measuring and interpreting neuronal correlations, Nat. Neurosci. **14**, 811 (2011).

[77] F. Gabbiani, Coding of time-varying signals in spike trains of linear and half-wave rectifying neurons, Network **7**, 61 (1996).

[78] F. Rieke, D. A. Bodnar, and W. Bialek, Naturalistic stimuli increase the rate and efficiency of information transmission by primary auditory afferents, Proc. R. Soc. London, Ser. A **262**, 259 (1995).

[79] A. B. Neiman and D. F. Russell, Sensory coding in oscillatory electroreceptors of paddlefish, Chaos **21**, 047505 (2011).

[80] R. D. Vilela and B. Lindner, Comparative study of different integrate-and-fire neurons: Spontaneous activity, dynamical response, and stimulus-induced correlation, Phys. Rev. E **80**, 031909 (2009).

[81] S. G. Sadeghi, M. J. Chacron, M. C. Taylor, and K. E. Cullen, Neural variability, detection thresholds, and information transmission in the vestibular system, J. Neurosci. **27**, 771 (2007).

[82] S. Blankenburg, W. Wu, B. Lindner, and S. Schreiber, Information filtering in resonant neurons, J. Comput. Neurosci. **39**, 349 (2015).

[83] H. Clague, F. Theunissen, and J. P. Miller, Effects of adaptation on neural coding by primary sensory interneurons in the cricket cercal system, J. Neurophysiol. **77**, 207 (1997).

[84] C. J. Rozell and D. H. Johnson, Examining methods for estimating mutual information in spiking neural systems, Neurocomputing **65**, 429 (2005).

[85] J. C. Roddey, B. Girish, and J. P. Miller, Assessing the performance of neural encoding models in the presence of noise, J. Comput. Neurosci. **8**, 95 (2000).